Journal of Sound and Vibration 329 (2010) 5105–5115

Contents lists available at ScienceDirect

Journal of Sound and Vibration

journal homepage: www.elsevier.com/locate/jsvi

Flexural vibrations of a rectangular plate for the lower normal modes

B. Manzanares-Martínez [a], J. Flores [b], L. Gutiérrez [c], R.A. Méndez-Sánchez [c,*], G. Monsivais [b], A. Morales [c], F. Ramos-Mendieta [d]

[a] División de Ciencias e Ingeniería, Universidad de Sonora. Blvd. Lazaro Cardenas #100, 85880 Navojoa, Sonora, Mexico
[b] Instituto de Física, Universidad Nacional Autónoma de México, A.P. 20-364, 01000 México, D.F., Mexico
[c] Instituto de Ciencias Físicas, Universidad Nacional Autónoma de México, A.P. 48-3, 62251 Cuernavaca, Morelos, Mexico
[d] Departamento de Investigación en Física, Universidad de Sonora, A.P. 5-088, 83000 Hermosillo, Sonora, Mexico

ARTICLE INFO

Article history:
Received 30 March 2009
Received in revised form
11 May 2010
Accepted 10 June 2010
Handling Editor: M.P. Cartmell
Available online 14 July 2010

ABSTRACT

Theoretical and experimental results for flexural waves of a rectangular plate with free ends are obtained. Both the natural frequencies and mode shapes are analyzed for the lower normal modes. To take into account the boundary conditions, a plane wave expansion method is used to solve the thin plate theory also known as the 2D Kirchhoff–Love equation. The excitation and detection of the normal modes of the out-of-plane waves are performed using non-contact electromagnetic-acoustic transducers. We conclude that this experimental technique is highly reliable due to the good agreement between theory and experiment.

1. Introduction

Vibrating plates are important in several engineering applications. Among many others, they are structural components of great importance; second, piezoelectric plates are used as oscillators in some electronic systems, and furthermore vibrating plates are also of importance in the analysis and construction of musical instruments. Therefore the normal modes of plates are of wide interest. For these reasons, extensive studies of the normal modes of plates of various shapes and for several boundary conditions have been performed. These studies are, however, mainly theoretical or numerical [1–5], and experimental studies are scarce [6–11]. The latter can be classified by the method used: X-ray diffraction topography [6], measurements with accelerometers or mechanical transducers [7,8], using TV-holographic systems, laser interferometry or speckle pattern interferometry [9–11]. Among these, the interferometric methods have the advantage of being non-contact techniques. However, additional work is needed to establish them as precise and controllable techniques [12].

We therefore perform the measurements with an electromagnetic-acoustic transducer (EMAT) which is very selective, made with commercial components and inexpensive. Compared with the interferometric methods these transducers have some advantages. For instance, to study in-plane oscillations our method requires only a slight change of the EMAT configuration used previously [13–17], whereas in the interferometric method a completely different configuration, i.e. the speckle configuration, is needed. Furthermore, our non-contact device can be used both as an exciter or as a detector, whereas in interferometric methods it is only the detection that is performed without any mechanical contact. Our method also gives directly the phases of the wave amplitudes. We therefore conclude that using the electromagnetic-acoustic transducers that we have developed is more efficient than the methods previously used in the study of vibrations of plates. We should point out, however, that our method requires a longer time for each measurement since a point by point

* Corresponding author. Tel.: +52 55 56 22 77 88; fax: +52 55 56 22 77 75.
E-mail address: mendez@fis.unam.mx (R.A. Méndez-Sánchez).

0022-460X/$ - see front matter © 2010 Elsevier Ltd. All rights reserved.
doi:10.1016/j.jsv.2010.06.010

scanning of the wave amplitudes must be done. This inconvenience can be circumvented using several EMATs that obtain the data simultaneously.

In this paper we employ the electromagnetic-acoustic transducers to measure the lower normal modes of the flexural vibrations of elastic plates. The EMATs are described in the next section. The experimental setup is also given there. In Section 3 the plane wave expansion (PWE) method is applied to the thin plate theory [18] since it is the simplest and most widely used theory of flexural vibrations in plates. This theory is also known as the Kirchhoff–Love theory [8] or simply as Kirchhoff theory [9]. We have obtained with this method the normal-mode frequencies and wave amplitudes of a rectangular plate. The results obtained with this method are compared with those calculated with other methods in the same section for both a rectangular and a square plate; two different boundary conditions are analyzed. In Section 4 the theoretical predictions of the plane wave expansion method are compared with the experimental measurements for an aluminum rectangular plate for the lower normal modes with free ends.

Although the results presented in this article appear to be specific, i.e. for a rectangular plate with free ends, they are also useful for many other systems. The experimental technique using EMATs has been applied to study several kinds of modes in rods with different shapes and it has been applied to the out-of-plane vibrations of a plate with any shape and boundary conditions. For instance, a measurement of the normal modes of a plate with the very irregular shape of the "ancient Tenochtitlan lake" has been measured [19]. A comparison between a wave amplitude using EMATs for this particular shape with their corresponding Chladni pattern is given in Section 2.

The plane wave expansion method, on the other hand, is a very popular numerical method among the photonic crystal community since the dispersion relation of specific photonic crystal geometries can be obtained easily. It has been applied to a plethora of undulatory systems. In particular it has been applied to several 2D acoustic systems [20–24]. This is a very important method since transport properties (bands, gaps, transmission, reflection coefficients, etc.) can be obtained using it. Furthermore, this method can be applied to finite systems by introducing them into a matrix of a second material with the appropriate boundary conditions (see below). In fact we will show in Section 3 that results for plates with clamped and free edges can be obtained.

2. Experimental setup to measure the frequency spectrum and the wave amplitudes

To excite the out-of-plane waves in the plates we use an electromagnetic-acoustic transducer developed recently to measure the vibration of beams [13–16]. This transducer measures the acceleration of the plate surface [14]. The transducer consists of a coil and a magnet and is highly selective to the different types of waves. The selection is done with different configurations of the coil and magnet. In the left-lower corner of Fig. 1 a sketch of the configuration used to excite the flexural waves is shown. A detailed explanation of the operation of these electromagnetic acoustic transducers through eddy currents and the different configurations of the coil and magnet is given in Refs. [13,14].

The frequency spectrum and the wave amplitudes were measured using a lock-in amplifier technique as can be seen in the setup of Fig. 1. The signal of an oscillator (Stanford Research Systems DS345) is amplified (Crown XTi 4000) and sent to

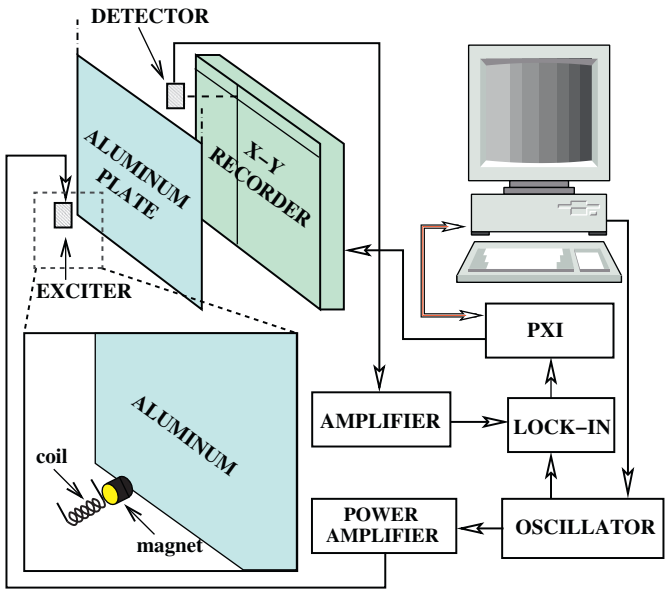

Fig. 1. Diagram of the experimental setup used to measure the frequency spectrum and wave amplitudes of the rectangular plate. The dashed line between the detector and the *X–Y* recorder indicates mechanical coupling. The dashed dotted lines indicate the threads supporting the plate. The coupling between the PXI and the computer is done through an optical fiber.

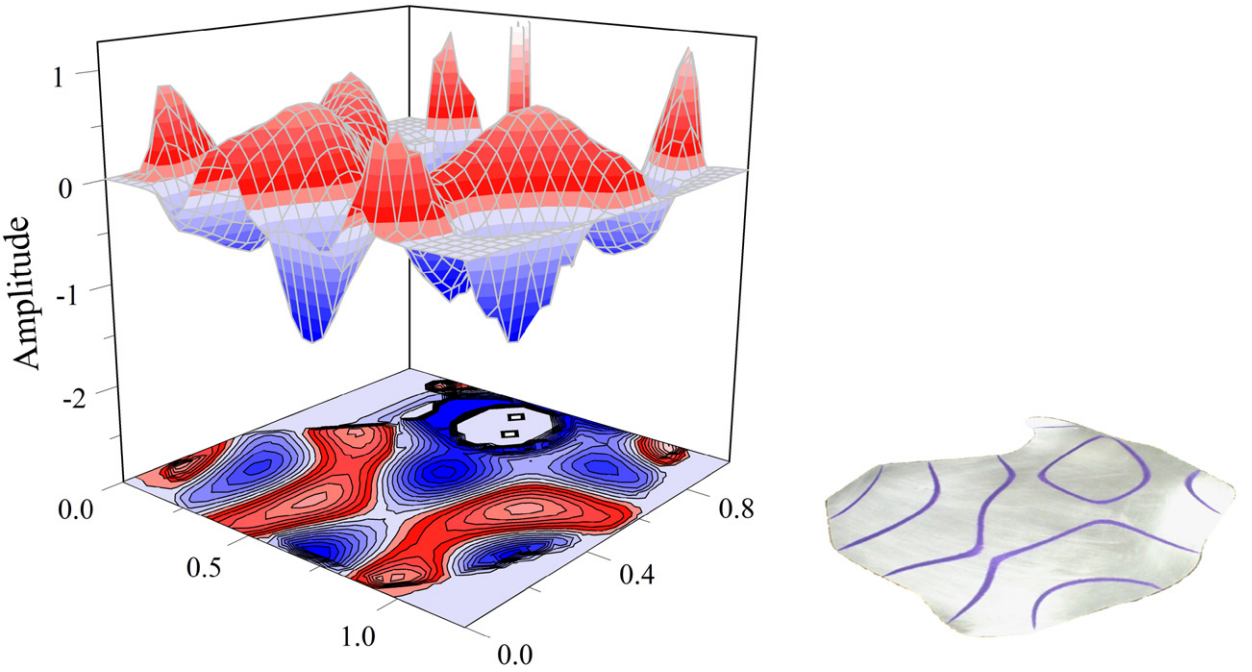

Fig. 2. Comparison between a measured wave amplitude with the EMATs (left) for a plate with the shape of the Tenochtitlan lake with the corresponding Chladni pattern (right).

the electromagnetic-acoustic transducer used as exciter. Another EMAT acts as a detector of the elastic vibrations. Its signal is sent to an amplifier (Stanford Research Systems SR560) and then to a lock-in amplifier (EG&G Princeton applied research 128A). The signal is then transmitted to a PXI of National Instruments and finally to a PC through an optical fiber (using a National Instruments PXI-8336 MXI-4 card). The reference signal of the lock-in was taken directly from the oscillator. The frequency of the oscillator is controlled by the computer through a port RS-232. To obtain the wave amplitudes the position of the detector is varied with a Hewlett-Packard 7004B *X–Y* recorder which is also controlled by the computer through the PXI. EMAT coils of diameters between 1 and 10 mm were used. For the results reported here, a coil with a diameter of 5 mm was used; this gives then the experimental spatial resolution. As seen in Fig. 1 the plates were supported vertically by two nylon threads glued to the plate's rim along its short side. The threads have negligible mass compared to that of the plate mass and they are very long so plate motions imply very small angles of the thread with respect to the vertical; therefore only negligible forces act on the plate due to the support. In any case the way the plate is supported does not affect the resulting measurements.

The computer programs were made with LabVIEW under Linux. One of the programs is dedicated to measure the frequency spectrum and another one, based on the first, to measure wave amplitudes. The variation of room temperature is controlled up to 0.5 K but this is not enough to prevent a temperature-dependent shift of the resonances. The program then obtains the resonance curve and determines its maximum value to measure the amplitude and frequency in real time. As an example we plot in Fig. 2 the comparison between a measured wave amplitude and its corresponding Chladni pattern for a plate with the shape of the ancient Tenochtitlan Lake on top of which downtown Mexico City is built [19]. The pattern was obtained by exciting the plate with the EMAT. Looking carefully at Fig. 2, one can see that the zero contour line obtained from the measurement with the EMAT agrees with the pattern notwithstanding that the plate has a very irregular shape. Note that the scanning is performed on a rectangular region and that the response is null outside the plate borders. Other modes show similar agreement with the Chladni patterns. Thus plates with irregular shapes can be measured easily with the EMATs. The maxima of the normal-mode wave amplitudes have typical values of 0.5 μm for frequencies around 3 kHz. The time τ for measuring a normal-mode wave amplitude with approximately 1000 points and one detector is $\tau \approx 20$ min. When the speed of the measurement is important more detectors can be added. Then the time is reduced by the number N of detectors as τ/N.

3. The plane wave expansion method for the Kirchhoff–Love equation

The equation that governs the out-of-plane wave motion in the thin plate theory is

$$\frac{\partial^2}{\partial x^2}\left[D\left(\frac{\partial^2 W}{\partial x^2}+\nu\frac{\partial^2 W}{\partial y^2}\right)\right]+2\frac{\partial^2}{\partial x\partial y}\left[D(1-\nu)\frac{\partial^2 W}{\partial x\partial y}\right]+\frac{\partial^2}{\partial y^2}\left[D\left(\frac{\partial^2 W}{\partial y^2}+\nu\frac{\partial^2 W}{\partial x^2}\right)\right]=-\rho h\frac{\partial^2 W}{\partial t^2}. \quad (1)$$

Here W is the flexural displacement in the z direction, v is the Poisson ratio and ρ the density of the plate. $D=Eh^3/12(1-v^2)$ is the flexural rigidity with E the Young modulus and h the thickness of the plate. Eq. (1) is a 2D generalization of the Bernoulli–Euler equation for the flexural vibrations of a beam [18].

In what follows a numerical method to calculate the normal modes of plates will be described. Following Refs. [20–22], a plane wave expansion (PWE) method will be used. The PWE method has the advantage that it can be used for 2D locally periodic systems like those of Refs. [21–23]. In the PWE method a unit rectangular cell of dimensions $a\times b$ is repeated periodically in the plane. The solutions for a rectangular plate with free-ends can be obtained by choosing a unit cell composed by the plate of interest in the center of the cell surrounded by a host material that mimics the vacuum (see Fig. 3). Plates with clamped edges can also be simulated taking a very rigid and dense host material but a modification to the programs is needed (see below).

The following expansions in the PWE method are assumed for D, Dv and ρh:

$$D=\sum_{\boldsymbol{G}}\alpha_{\boldsymbol{G}}\exp(\mathrm{i}\boldsymbol{G}\cdot\boldsymbol{r}), \tag{2}$$

$$Dv=\sum_{\boldsymbol{G}}\beta_{\boldsymbol{G}}\exp(\mathrm{i}\boldsymbol{G}\cdot\boldsymbol{r}), \tag{3}$$

$$\rho h=\sum_{\boldsymbol{G}}n_{\boldsymbol{G}}\exp(\mathrm{i}\boldsymbol{G}\cdot\boldsymbol{r}). \tag{4}$$

Here $\boldsymbol{r}=(x,y)$ and $\boldsymbol{G}=(G_x,G_y)=((2\pi/a)p,(2\pi/b)q)$ is a reciprocal vector where p and q are integers. For the flexural displacement it is assumed that

$$W(\boldsymbol{r},t)=\exp(\mathrm{i}\boldsymbol{k}\cdot\boldsymbol{r}-\omega t)\sum_{\boldsymbol{G}}\phi_{\boldsymbol{G}}\exp(\mathrm{i}\boldsymbol{G}\cdot\boldsymbol{r}), \tag{5}$$

where $\boldsymbol{k}$ is the wave vector and ω the angular frequency. Inserting the expansions of Eqs. (2)–(5) in Eq. (1) one gets

$$\sum_{\boldsymbol{G}'}\{\alpha_{\boldsymbol{G}-\boldsymbol{G}'}[(k_x+G_x')(k_x+G_x)+(k_y+G_y')(k_y+G_y)]^2+\beta_{\boldsymbol{G}-\boldsymbol{G}'}[(k_x+G_x)(k_y+G_y')-(k_x+G_x')(k_y+G_y)]^2\}\phi_{\boldsymbol{G}'}=\omega^2\sum_{\boldsymbol{G}'}n_{\boldsymbol{G}-\boldsymbol{G}'}\phi_{\boldsymbol{G}'} \tag{6}$$

for each $\boldsymbol{G}$. This is a generalized eigenvalue equation:

$$\mathbb{M}\Phi=\omega^2\mathbb{N}\Phi, \tag{7}$$

where Φ is a vector with entries $\phi_{\boldsymbol{G}'}$. $\mathbb{M}$ and $\mathbb{N}$ are infinite matrices with entries

$$\mathbb{M}(\boldsymbol{G},\boldsymbol{G}')=\alpha_{\boldsymbol{G}-\boldsymbol{G}'}[(\boldsymbol{k}+\boldsymbol{G})\cdot(\boldsymbol{k}+\boldsymbol{G}')]^2+\beta_{\boldsymbol{G}-\boldsymbol{G}}[(k_x+G_x)(k_y+G_y')-(k_x+G_x')(k_y+G_y)]^2 \tag{8}$$

and

$$\mathbb{N}(\boldsymbol{G},\boldsymbol{G}')=n_{\boldsymbol{G}-\boldsymbol{G}'}. \tag{9}$$

As can be seen from Eqs. (2)–(4), $\alpha_{\boldsymbol{G}}$, $\beta_{\boldsymbol{G}}$ and $n_{\boldsymbol{G}}$ are the Fourier coefficients of the expansion of the parameters D, Dv, and ρh, respectively. They are functions of $\boldsymbol{r}$ (see Fig. 3), so that the solutions for a rectangular plate with free-ends can be obtained by defining a unit cell with a plate in the center surrounded by a material that mimics the vacuum, as was mentioned above. This material is defined with D_2 fixed and $\rho_2\to 0$ [24,25]. The resulting eigenvalue equation is then solved with standard LAPACK routines. The Fourier coefficients can be calculated analytically for the plate of Fig. 3. Plates with irregular shape can also be calculated but in this case the Fourier coefficients should be obtained numerically. In principle the sum in Eqs. (2)–(4) should include an infinite number of plane waves; in practice a large but fixed number of plane waves is used. The convergence of the numerical solutions as a function of the number of plane waves will be given in the next section.

The usefulness of the plane wave expansion method will be shown first by calculating some plates that have been calculated and/or measured previously [7] and second by comparing the numerical results with our experimental measurements, which will be done in the next section.

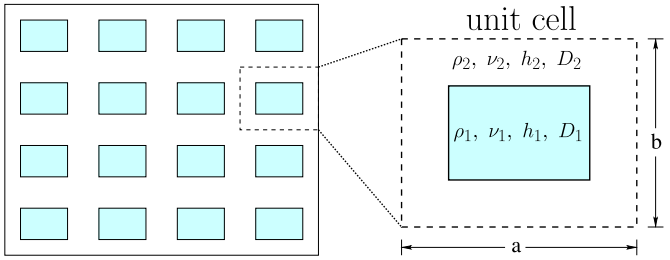

Fig. 3. Scheme of the system calculated with the plane wave expansion method. A rectangular cell of length sides a and b is repeated periodically in the plane. The plate of interest of material I is located in the center of the cell surrounded by material II that fills the cell and mimics the vacuum for free edges or a very rigid and dense material for clamped edges.

Table 1
Normal mode frequencies of a rectangular plate of 254 mm × 381 mm and thickness h=1.59 mm with free ends.

Plane wave expansion		Analdyne-1		Leissa		Singal, Gorman and Forgues	
Mode	(Hz)	(Hz)	%Error	(Hz)	%Error	(Hz)	%Error
1	52.7	52.88	0.34	54.21	2.87	49.48	6.11
2	56.75	57.04	0.51	58.17	2.50	54.60	3.79
3	122.03	122.57	0.44	125.63	2.95	117.36	3.83
4	133.32	134.00	0.51	135.43	1.58	132.18	0.86
5	152.29	152.94	0.43	156.73	2.92	146.63	3.72
6	179.22	180.19	0.54	181.75	1.41	176.00	1.80

The results obtained with the plane wave expansion method are compared with other methods. The material constants are those of the aluminum: Young modulus E=69 GPa and density $\rho = 26.85\ \mathrm{kN/m^3}$.

Table 2
Normal mode frequencies of a square plate of 254 mm × 254 mm and thickness h=1.59 mm with free ends.

Plane wave expansion		Analdyne-1		Leissa		Singal, Gorman and Forgues	
Mode	(Hz)	(Hz)	%Error	(Hz)	%Error	(Hz)	%Error
1	79.47	79.79	0.40	81.84	2.98	78.79	0.86
2	115.99	116.48	0.42	119.91	3.38	117.28	1.11
3	147.01	147.99	0.67	148.03	0.69	144.85	1.47
4	206.29	207.42	0.55	212.2	2.86	203.66	1.27
5	206.49	207.42	0.45	212.2	2.77	205.67	0.40
6	367.06	369.13	0.56	372.83	1.57	364.65	0.66

The results obtained with the plane wave expansion method are compared with other methods. The material constants are those of the aluminum: Young modulus E=69 GPa and density $\rho = 26.85\ \mathrm{kN/m^3}$.

Table 3
Normal mode frequencies of a rectangular plate (with clamped ends) of 300 mm × 600 mm and thickness h=2 mm obtained with the plane wave expansion method and its comparison with published results.

Plane wave expansion		Holography		Shaker		Leissa	
Mode	(Hz)	(Hz)	%Error	(Hz)	%Error	(Hz)	%Error
1	134.49	127.8	4.97	136.3	1.35	137.96	2.58
2	174.01	145.7	16.27	151.3	13.05	178.67	2.68
3	244.81	227.7	6.99	227.5	7.07	251.42	2.70
4	346.27	289.8	16.31	322.5	6.86	355.61	2.70
5	349.83	284.9	18.56	338.8	3.15	359.19	2.68
6	388.62	343.9	11.51	351.8	9.47	399.15	2.71
7	455.3	396.8	12.85	411.3	9.66	468.11	2.81
8	477.09	454.5	4.73	473.8	0.69	566.5	18.74
9	551.01	546.4	0.84	573.8	4.14	692.22	25.63
10	636.19	632.9	0.52	666.3	4.73	732.14	15.08
11	673.97	684.9	1.62	736.3	9.25	800.75	18.81

First we study normal modes of plates with all edges free. In Table 1 we show the normal mode frequencies of a rectangular plate of 254 mm × 381 mm and thickness h=1.59 mm with free ends obtained with the PWE method. The experimental results by Singal et al. [26] and their numerical values using the program designated Analdyne-1 as well as the calculations by Leissa [1] are also shown. The percent errors, taking as reference the results obtained with the PWE method, are also given in the same table. As can be seen the best agreement of the PWE method is obtained with the program Analdyne-1. The larger errors, about ~ 7 percent, are obtained in the comparison with the Singal, Gorman and Forgues experimental results.

In Table 2 we show the normal mode frequencies of a square plate of 254 mm × 254 mm and thickness h=1.59 mm with free ends. As can be seen, the results obtained with the PWE method show very good agreement with the results of Ref. [26] and with the results of their calculation using the program Analdyne-1. The results of Leissa [1] present percent errors of less than 3.4 percent when compared with the PWE method.

To simulate a plate with clamped edges a unit cell is formed by the rectangular plate in the center surrounded by a material with fixed flexural rigidity D and $\rho \to \infty$. Unfortunately the PWE method described above has serious convergence

Table 4
Normalized normal mode frequencies of a square plate of 300 mm × 600 mm and thickness h=2 mm with clamped ends.

Plane wave expansion		Polynomial quadrature differential method		Leissa	
Mode	Normalized frequency	Normalized frequency	%Error	Normalized frequency	%Error
1	36	35.598	1.12	35.992	0.02
2=3	73.394	73.394	0.00	73.413	0.03
4	108.22	108.217	0.00	108.27	0.05
5	131.581	131.581	0.00	131.64	0.04
6	132.23	–	–	132.24	0.01

The data are normalized according to $\Omega = \omega a^2 \sqrt{\rho h/D}$. Mode 6 is not available by polynomial quadrature differential method.

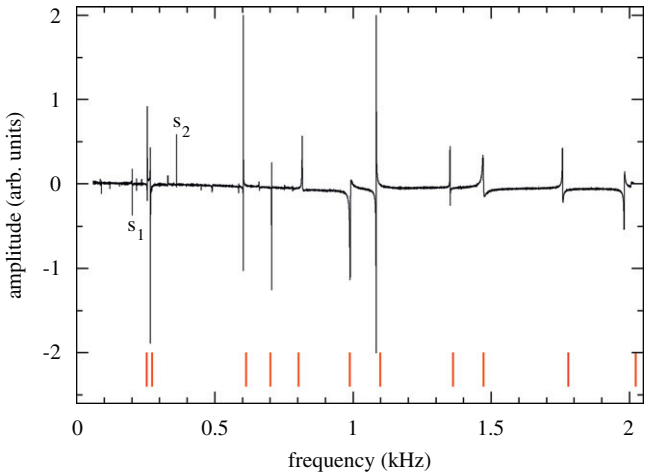

Fig. 4. Spectrum of the rectangular plate of 203 mm × 355 mm × 6.12 mm obtained with the EMATs. The vertical lower lines correspond to the theoretical predictions.

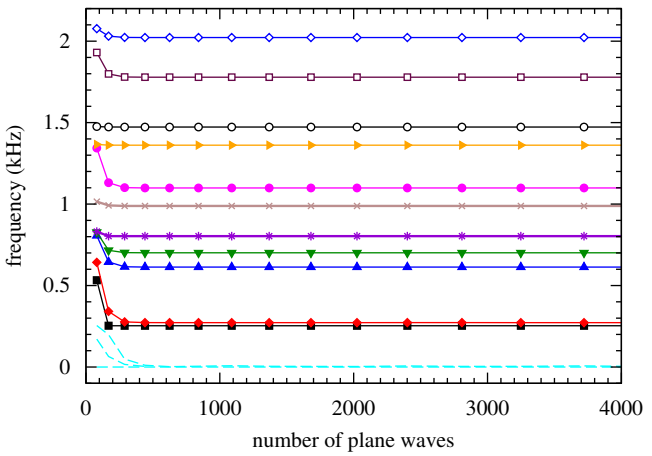

Fig. 5. Convergence of the plane wave expansion method. The three lowest (cyan) lines correspond to the movement of the plate at a constant velocity at zero frequency. Modes 1–11 of Table 5 appear in increasing order above the cyan lines.

problems with this unit cell due to the large elastic mismatch. Then, following Cao et al. [27], we implement a different strategy by using an inverse Fourier factorization of products. This technique was utilized in Ref. [22] to study the flexural vibrations of thin plates with locally resonant structures. The results obtained with this technique for a rectangular plate of 600 mm × 300 mm are given in Table 3. In the same table the results of experiments with a shaker [7], with an holographic method [7] and those of Leissa [1] are also given. Here we have two different experimental results. To calculate the percent errors, instead of using the experimental values as the true values, we will use as true value the results of the PWE method. In this case the percent errors are larger than in the case of the plate with free-edges. The normal modes of a square plate with all ends clamped were also computed with the PWE method; the results for the six lower modes are given in Table 4.

Table 5
Frequencies of a rectangular plate of 203 mm × 355 mm and thickness h=6.12 mm.

Mode number N	Classification	Experimental frequency f_N^E (Hz)	Theoretical frequency f_N^T (Hz)
1	(2, 0)	255.5	253.3
2	(1, 1)	266.8	272.4
3	(2, 1)	602.9	613.2
4	(3, 0)	705.3	701.0
5	(0, 2)	815.9	803.2
6	(1, 2)	989.3	988.5
7	(3, 1)	1083.6	1098.9
8	A	1350.8	1361.6
9	B	1470.4	1471.5
10	(4, 1)	1758.0	1778.8
11	(3, 2)	1981.0	2022.1

The pairs (n,m) represent the number of nodal lines in the long (n) and short (m) sides, respectively. For modes labelled "A" and "B" this classification does not apply.

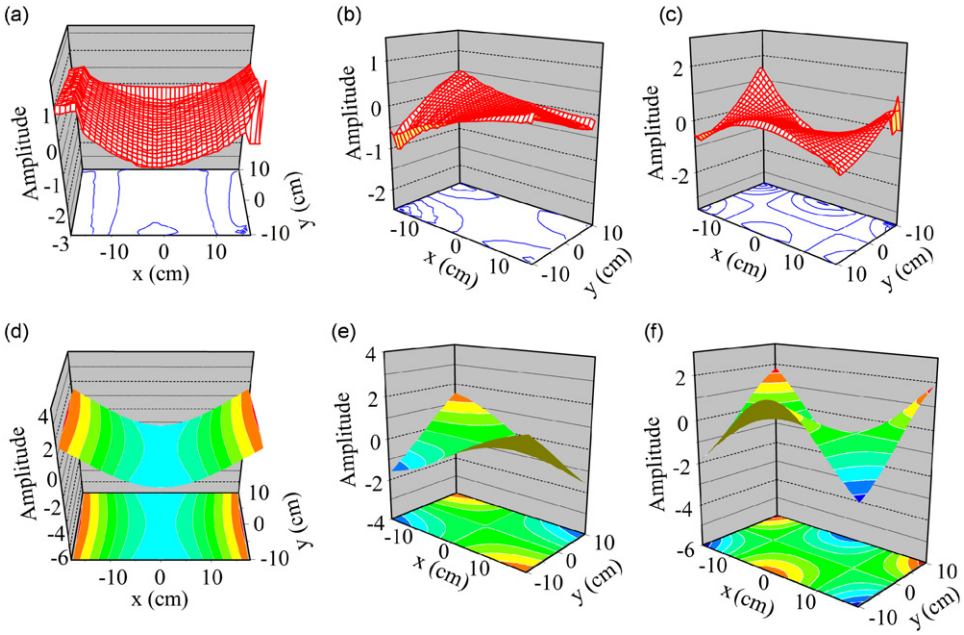

Fig. 6. Normal-mode amplitudes (in arbitrary units) for flexural waves of the rectangular plate. The upper parts, i.e., (a), (b), and (c), are experimental results. The lower part, i.e., (d), (e), and (f), corresponds to theoretical amplitudes. The modes from left to right correspond to the (2,0), (1,1) and (2,1) modes of Table 5.

The results of the polynomial quadrature differential method [28] and those of Leissa are also given. One can notice that, with the exception of one mode, the percent errors are smaller than 0.06 percent.

4. Comparison between theory and experiment

In Fig. 4 the spectrum obtained for a rectangular plate of 203 mm × 355 mm and thickness h=6.12 mm is shown. To perform this measurement the exciter and detector were located at the right and left lower corners of the plate, respectively. In the theoretical calculations the values $E=68\times10^9\,\mathrm{N/m^2}$, $\rho=2699\,\mathrm{kg/m^3}$ and $\nu=0.33$ were used and we have taken 3721 plane waves into account. As can be seen in this figure the theoretical normal-mode frequencies agree with the experimental one but the difference between theory and experiment grows with frequency. This is expected since the Kirchhoff–Love model does not take into account the effects of the rotary inertia nor of shear forces. The convergence of the solutions can be observed in Fig. 5. It was probed by increasing the number of plane waves. As can be seen they already converge for 500 waves. We used 3721 plane waves obtaining variations of less than 1 percent. In Table 5 we show the experimental f_N^E as well as the theoretical f_N^T frequencies we have obtained. The difference between theory and experiment is less than 3 percent.

It can be observed in Fig. 4 that there are some small peaks at frequencies below 800 Hz not predicted by the theory. This effect is known [29] and it was found previously in the study of uniform rods [13]. These peaks are subharmonics of

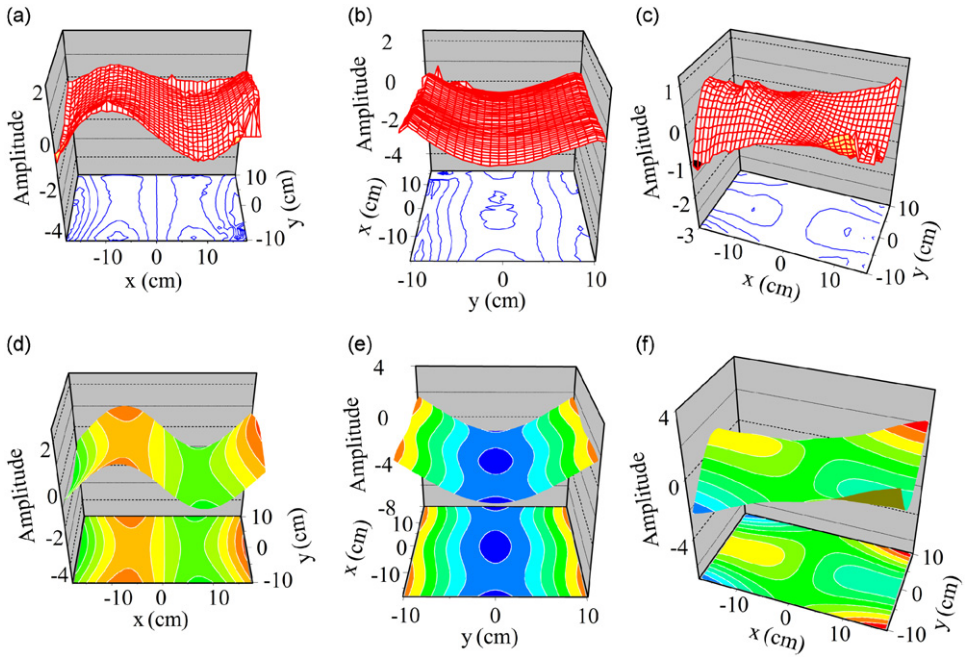

Fig. 7. Normal-mode amplitudes (in arbitrary units) of flexural waves in the rectangular plate. The upper part corresponds to experimental amplitudes ((a), (b), and (c)). The lower parts are theoretical results ((d), (e), and (f)). The modes from left to right correspond to the (3,0), (0,2) and (1,2) modes of Table 5.

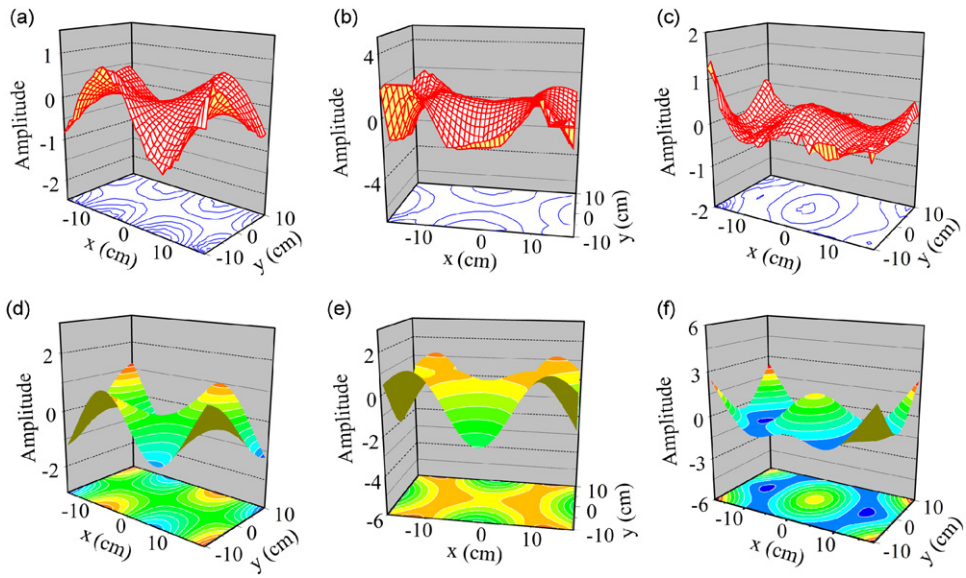

Fig. 8. Normal-mode amplitudes (in arbitrary units) of flexural waves in the rectangular plate. The upper part corresponds to experimental amplitudes ((a), (b), and (c)). The lower parts are theoretical results ((d), (e), and (f)). The modes from left to right correspond to modes (3,1), A and B of Table 5. Notice that modes A and B cannot be classified according to the number of vertical and horizontal nodal lines.

some of the frequencies given in Table 5. For instance, there are two noticeable peaks S_1 and S_2, one at $f_{S_1} \approx 201$ Hz and another one at $f_{S_2} \approx 361$ Hz. In fact, $f_{S_1} = \frac{1}{3} f_3^E$ and $f_{S_2} = \frac{1}{3} f_7^E$. We have verified that several subharmonics appear with very small amplitudes.

A comparison between the theoretical and the experimental wave amplitudes is given in Figs. 6–9. These wave amplitudes correspond to all modes given in Table 5. The experimental wave amplitudes were measured on a rectangular grid of 42 points in the *X*-axis times 24 points in the *Y*-axis. In these figures one can notice that some wave amplitudes can

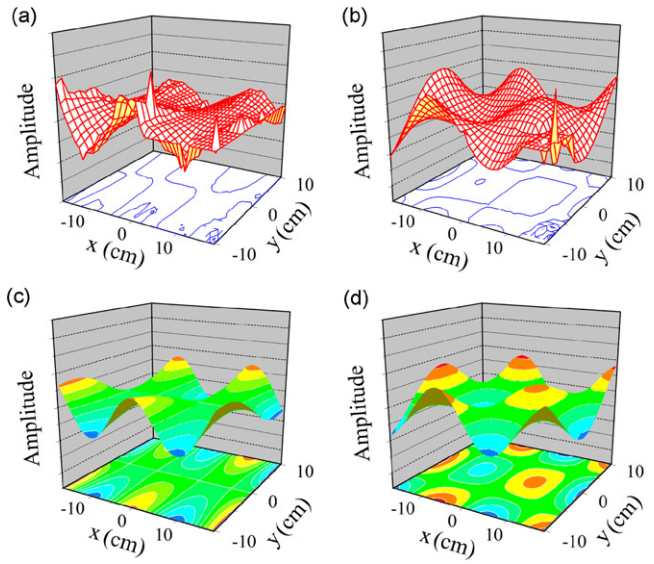

Fig. 9. Normal-mode amplitudes (in arbitrary units) of flexural waves in the rectangular plate. The upper part, (a) and (b), corresponds to experimental amplitudes. The lower parts, (c) and (d), are theoretical results. The modes from left to right correspond to modes (4,1), and (3,2) of Table 5.

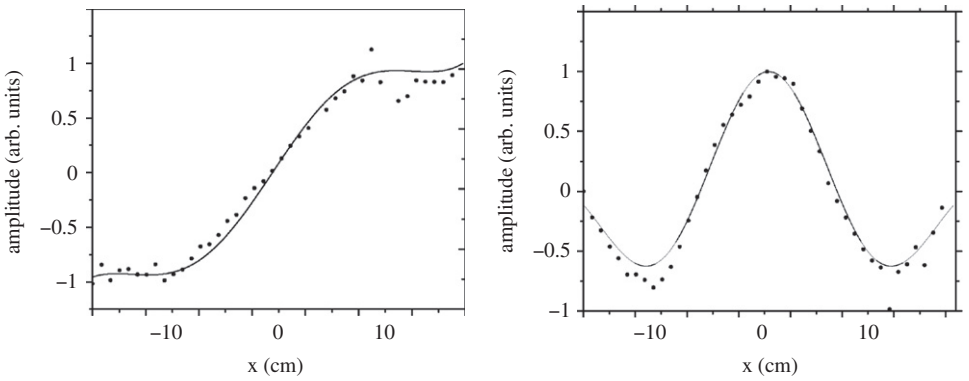

Fig. 10. Cuts of the normal-mode wave amplitudes of Figs. 7 and 8 across a central line in the long side; left, mode (1,2) and right, mode B.

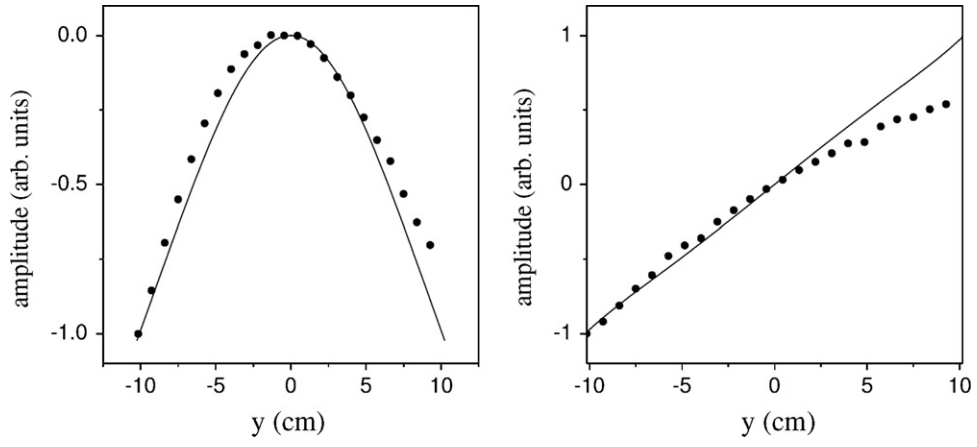

Fig. 11. Cuts of the normal-mode wave amplitudes of Figs. 7 and 8 at (a) $x=-13.42$ cm, mode (1,2), and (b) $x=6.5$ cm, mode (3,1).

be labelled by pairs of numbers (n,m), where n and m are the number of nodal lines in the long and short sides of the plate, respectively. This is done notwithstanding that the nodal lines are not completely vertical nor horizontal. Other modes, like modes A and B of Table 5, shown in the right and center of Fig. 8, cannot be labelled in this way. One can also see that the wave amplitudes are disturbed at the right-lower corner of the plate. It is here that the exciter is located and its magnetic field saturates the coil of the electromagnetic acoustic transducer used as detector.

As a first impression, from Figs. 6 to 9 one can say that the agreement between theory and experiment is excellent. However, a more quantitative study shows some small differences. This study can be made by plotting cuts parallel to the plate faces. In Figs. 10 and 11 some cuts of the wave amplitudes shown in Figs. 7 and 8 across both sides of the plate are shown. Figs. 10(a) and (b) correspond to cuts along the long side at the center of modes (1,2) and B, respectively. The cuts given in Figs. 11(a) and (b) are along the short side at fixed x of modes (1,2) and (3,1), respectively. These figures show a reasonable agreement between theory and experiment.

5. Conclusions

We have studied theoretically and experimentally the flexural vibrations of a rectangular aluminum plate with free ends. The experiments were made using electromagnetic-acoustic transducers—that seem to be well suited for this purpose—and for the theoretical calculations the plane wave expansion method was used. For the lower normal modes, within the range of 0.25–2 kHz, the agreement between theory and experiment is very acceptable, with differences less than 3 percent. Our experimental data deliver directly the amplitude of the out-of-plane displacement. We have presented a series of 3D plots with the theoretical and experimental displacement profiles; cuts of these images show slight deviations at points near the location of the exciter.

Acknowledgements

This work was supported by UNAM DGAPA PAPIIT projects IN111308 and IN116206, by Subsecretaría de Educación Superior e Investigación Científica, México, Programa de Mejoramiento del Profesorado, special Grant "Redes de Cuerpos Académicos 2004" and by CONACyT, México Grant nos. SEP-2004-C01-47636 and 50308-F.

References

[1] A.W. Leissa, *Vibration of Plates*, Vol. 1, Acoustical Society of America, Woodbury, NY, 1993, p. 115.
[2] W. Soedel, *Vibrations of Shells and Plates*, Marcel Dekker, New York, 1993.
[3] R. Szilard, *Theory and Analysis of Plates: Classical and Numerical Methods*, Prentice-Hall, Englewood Cliffs, NJ, 1974.
[4] D.J. Gorman, *Vibration Analysis of Plates by the Superposition Method, Series on Stability Vibrations and Control of Systems*, Vol. 3, World Scientific, Singapore, 1999.
[5] N.S. Bardell, Chladni figures for completely free parallelogram plates: an analytical study, *Journal of Sound and Vibration* 174 (1994) 655–676.
[6] P.C.Y. Lee, W.J. Spencer, Shear-flexure-twist vibrations in rectangular *AT*-cut quartz plates with partial electrodes, *Journal of the Acoustical Society of America* 45 (1969) 637–645.
[7] K.H. Low, G.B. Chai, T.M. Lim, S.C. Sue, Comparisons of experimental and theoretical frequencies for rectangular plates with various boundary conditions and added masses, *International Journal of Mechanical Sciences* 40 (1998) 1119–1131.
[8] K. Schaadt, T. Guhr, C. Ellegaard, M. Oxborrow, Experiments on elastomechanical wave functions in chaotic plates and their statistical features, *Physical Review E* 68 (2003) 036205.
[9] F.J. Nieves, F. Gascón, A. Bayón, Natural frequencies and mode shapes of flexural vibration of plates: laser-interferometry detection and solutions by Ritz's method, *Journal of Sound and Vibration* 278 (2004) 637–655.
[10] C.C. Ma, C.C. Lin, Experimental investigation of vibrating laminated composite plates by optical interferometry method, *American Institute of Aeronautics and Astronautics Journal* 39 (2001) 491–497.
[11] C.C. Ma, H.Y. Lin, Experimental measurements on transverse vibration characteristics of piezoceramic rectangular plates by optical methods, *Journal of Sound and Vibration* 286 (2005) 587–600.
[12] B.E. Olivos-Fuentes, L. Gutiérrez, A. Morales, Real time interferometric measurement of the parameters of a mechanical oscillator, *Review of Scientific Instruments* 69 (1998) 3435–3436.
[13] A. Morales, L. Gutiérrez, J. Flores, Improved eddy current driver-detector for elastic vibrations, *American Journal of Physics* 69 (2001) 517–522.
[14] A. Morales, J. Flores, L. Gutiérrez, R.A. Méndez-Sánchez, Compressional and torsional wave amplitudes in rods with periodic structures, *Journal of the Acoustical Society of America* 112 (2002) 1961–1967.
[15] R.A. Méndez-Sánchez, A. Morales, J. Flores, Experimental check on the accuracy of the Timoshenko's beam theory, *Journal of Sound and Vibration* 279 (2005) 508–512.
[16] A. Díaz-de-Anda, A. Pimentel, J. Flores, A. Morales, L. Gutiérrez, R.A. Méndez-Sánchez, Locally periodic Timoshenko rod: experiment and theory, *Journal of the Acoustical Society of America* 117 (2005) 2814–2819.
[17] L. Gutierrez, A. Diaz-de-Anda, J. Flores, R.A. Mendez-Sanchez, G. Monsivais, A. Morales, Wannier-Stark ladders in one-dimensional elastic systems, *Physical Review Letters* 97 (2006) 114301.
[18] K.F. Graff, *Wave Motion in Elastic Solids*, Dover, New York, 1991, p. 233.
[19] J. Flores, Nodal patterns in the seismic response of sedimentary valleys, *European Physical Journal—Special Topics* 145 (2007) 63–75.
[20] M.M. Sigalas, E.N. Economou, Elastic waves in plates with periodically placed inclusions, *Journal of Applied Physics* 75 (1994) 2845–2850.
[21] D. Yu, Y. Liu, J. Qiu, G. Wang, H. Zhao, Complete flexural vibration band gaps in membrane-like lattices structures, *Physics Letters A* 357 (2006) 154–158.
[22] D.-L. Yu, G. Wang, Y.-Z. Liu, Y.-H. Wen, J. Qiu, Flexural vibration band gaps in thin plates with two-dimensional binary locally resonant structures, *Chinese Physics* 15 (2006) 0266–0271.
[23] J.-C. Hsu, T.-T. Wu, Efficient formulation for band-structure calculations of two-dimensional phononic-crystal plates, *Physical Review B* 74 (2006) 144303.

[24] B. Manzanares-Martínez, F. Ramos-Mendieta, Sagittal acoustic waves in phononic crystals: k-dependent polarization, *Physical Review B* 68 (2003) 134303.
[25] J.O. Vasseur, P.A. Deymier, B. Djafari-Rouhani, Y. Pennec, A.-C. Hladky-Hennion, Absolute forbidden bands and waveguiding in two-dimensional phononic crystal plates, *Physical Review B* 77 (2008) 085415.
[26] R.K. Singal, D.J. Gorman, S.A. Forgues, A comprehensive analytical solution for free vibration of rectangular plates with classical edge conditions: experimental verification, *Experimental Mechanics* 32 (1992) 21–23.
[27] Y. Cao, Z. Hou, Y. Liu, Convergence problem of plane-wave expansion method for phononic crystals, *Physics Letters A* 327 (2004) 247–253.
[28] A. Krowiak, Methods based on the differential quadrature in vibration analysis of plates, *Journal of Theoretical and Applied Mechanics* 46 (2008) 123–139.
[29] K.R. Symon, *Mechanics*, Addison-Wesley Publishing Company, Reading, MA, 1971, p. 60.